Electronic Research Archive

ERA, 31(4): 1982–1997.
DOI: 10.3934/era.2023102
Received: 12 December 2022
Revised: 22 January 2023
Accepted: 25 January 2023
Published: 14 February 2023

http://www.aimspress.com/journal/ERA

Research article

Multi-objective optimization design for steel-aluminum lightweight body of pure electric bus based on RBF model and genetic algorithm

Wuhua Jiang*, Yuexin Zhang, Jie Liu, Daisheng Zhang, Yajie Yan and Chuanzheng Song

School of Automotive and Transportation Engineering, Hefei University of Technology, Hefei 230009, China

* **Correspondence:** Email: whjiang@hfut.edu.cn.

Abstract: In order to solve the problem of insufficient range caused by the excessive weight of the pure electric bus, a multi-objective genetic algorithm (GA) and radial basis function (RBF) model are combined in this paper to realize the lightweighting of steel and aluminum hybrid body of the pure electric bus. First, the upper and lower frames of the pure electric bus body are initially designed with aluminum alloy and steel materials respectively to meet the lightweight requirements. Second, a finite element (FE) model of the bus body is established, and the validity of the model is validated through physical tests. Then, the sensitivity analysis is performed to identify the relative importance of individual design parameters over the entire domain. The Hamosilei sampling method is selected for the design of the experiment (DOE) because users can specify the number of experiments and ensure that the set of random numbers is a good representative of real variability, and the RBF model is adopted to approximate the responses of objectives and constraints. Finally, the multi-objective optimization (MOO) method based on GA with RBF model is used to solve the optimization problem of the lightweight steel-aluminum hybrid bus body. The results show that compared with the traditional fully steel body, the use of the aluminum alloy lower-frame structure can reduce body mass by 38.4%, and the proposed optimization method can further reduce the mass of the steel-aluminum body to 4.28% without affecting the structural stiffness and strength performance of the body.

Keywords: pure electric bus; multi-objective optimization design; lightweight; steel-aluminum body

1. Introduction

Range anxiety has become an urgent problem for pure electric buses in recent years. The Lightweight of the bus is one of the effective solutions to this problem. The way of bus lightweight mainly depended on the use of lightweight materials, advanced manufacturing processes and structural optimization [1]. Among the lightweight materials, aluminum alloy was widely used in the lightweight design of the bus body structure due to its low mass and high performance [2]. Structural optimization methods are one of the main research directions of lightweight design, and these methods, including size and shape optimization methods, have previously been applied in structural design [3,4]. Topology optimization has always been the most promising and widely used structural optimization method in lightweight design [5,6]. X. Xu et al. [6] proposed and analyzed a series of variable-thickness honeycombs with enhanced bionic cells (VTHEBs). Compared with conventional structures, the VTHEBs had better material distribution, which could help to improve the crushing force level and energy absorption potential.

In the process of structural lightweight design, it is difficult to meet the strength and stiffness requirements of the body only by optimizing a single variable, which will seriously affect the safety of the bus. In order to improve the performance of multiple objectives by considering multiple design variables at the same time, a MOO problem could be formulated to seek the best possible value of design variables that could solve the optimization problem of body structure [7–10]. A. Ariyarit et al. [8] used multi-objective GA such as NSGA-II in conjunction with the FE method to analyze the structure and solve the optimal design of an automated guided vehicle (AGV) structure as a MOO problem. However, due to the complexity of this approach, searching for the optimal solution in the design space requires a large number of simulations and will ignore possible interaction effects between parameters. To address these problems, some potential methods are proposed by combining approximate model technology and a heuristic search algorithm. For example, Z. Xiang and Z. Zhu [9] reduced the complexity of multi-objective GA by using response surface methodology (RSM) to derive approximate regression models for stress ranges of fatigue details and structural weights. Z. Zhang et al. [10] proposed a MOO model of lubricant volume that takes the effects of temperature and heat into account to determine the lubrication volume of transmission components by taking the electronically controlled limited slip differential (ELSD) of an automobile as the research object. With the development of computers, the use of RBF models is also increasing. Y. Ji et al. [11] used RBF neural networks to fit the relationship between the mapping of variables and targets, increasing the efficiency of the optimized model.

The sensitivity analysis and optimization design of a 12 meters long pure electric bus with a load-carrying body using different materials for upper and lower frames are studied in this paper. Considering that the main load-carrying parts of the bus are located in the lower-frame, the structure is made of steel; since the upper-frame does not need to carry heavy loads, the structure is designed with aluminum alloy materials. After determining the materials of the body structure components, the FE model of the body structure is established, and the validity of the model is verified by physical test results. In order to further reduce the body mass and improve the structural stiffness and strength performance, sensitivity analysis is used to select the design variables; and the MOO method based on the RBF model and GA is used to seek the optimal design solution.

2. Establishment of FE model

In this paper, the body structure of a pure electric full-load city bus with a length of 12 meters is designed using a modular design method. The structure of the full-load bus body consists of two parts: the upper-frame and lower-frame, whereas the upper-frame consists of five parts: the front and rear enclosures, the left and right enclosures and the top cover. The biggest difference between the pure electric bus and the traditional fuel bus is the power system. The power battery of the pure electric bus is primarily located in the middle and rear of the lower-frame, and the motor is rear-mounted. Therefore, the newly designed bus body upper-frame follows the traditional fuel bus skeleton structure, but the aluminum alloy 6061-T6 material is applied instead of steel. Compared with the all-steel structure, the upper-frame mass is reduced from 3905 to 2404 kg, with a lightweight ratio of 38.4%.

The central and rear parts of the lower-frame structure were designed separately and made of 16Mn, high-strength steel, because this part of the structure is the main load-carrying part of the power cell. Due to the different materials used between the side surrounds and the lower-frame, there are many discussions about the connection methods between dissimilar materials [12,13], and the bolt riveting method was chosen for the connection after comprehensive consideration. Finally, the modules were assembled and connected, and the three-dimensional geometric model of the entire bus body skeleton structure with the combination of steel and aluminum was built. As shown in Figure 1, the upper-frame structure of the body is made of aluminum alloy, while the load-carrying structure of the lower-frame of the body is made of steel.

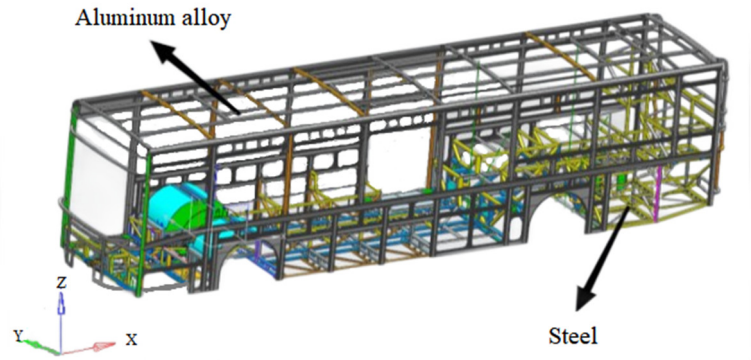

Figure 1. Three-dimensional model of pure electric bus body structure.

The three-dimensional geometric model of steel-aluminum body structure of the pure electric bus is imported into the Hypemesh software for FE modeling. When the modules are assembled, the welded joints on the body are handled by merging nodes. And for the bolt riveting, a method considering the contact of solid element named after PSOLID, plate and shell element named after PSHELL and rigid element named after RBE2 is proposed in this paper. The processing results of the two connection methods are shown in Figure 2.

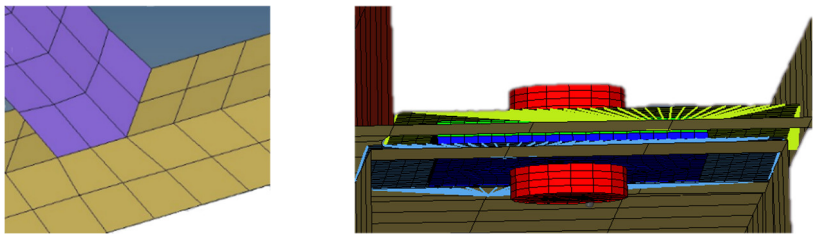

Figure 2. Handling of welded and bolted riveted joints.

Air springs are used in the front and rear suspension systems of the bus to reduce vibration. Although air spring have a lower mass than other springs, their size is larger and their structure is more complex. To reduce the difficulty of FE modeling, the spring unit named after CELAS1 was used to approximate the spring, then the rigid unit named after RBE2 was applied to couple the spring unit and simplify the axle. Figure 3 depicts the equivalent air spring suspension that was established.

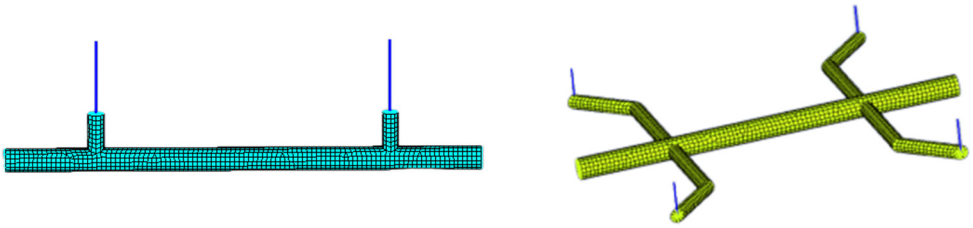

Figure 3. Equivalent air spring suspension.

Set the mass points of the motor and steering gear at the mass center, and then apply the RBE2 unit to the corresponding nodes. For distributed mass such as power battery and air conditioner, the mass unit is applied to the corresponding nodes of the body frame in a distributed way. The FE model of the bus skeleton is shown in Figure 4. The model contains 1,168,878 nodes and 1,084,295 shell elements.

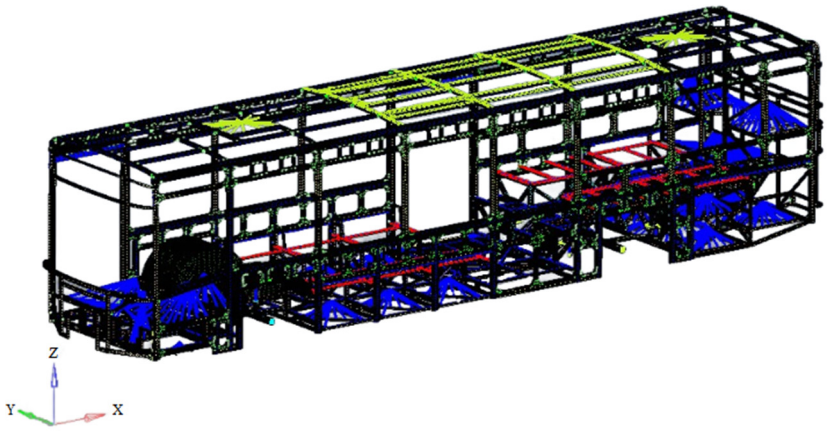

Figure 4. FE model of bus body frame.

3. Validation of the FE model

In order to verify the accuracy of the established FE model, a static electric physical test on the steel-aluminum combination bus body skeleton structure is conducted in this paper. According to the results of the FE analysis, 100 measuring points with large deformation are selected on the bus body skeleton.

Figure 5 shows the positions and serial numbers of some measuring points on the frame. Apply load at the installation positions of the frame, power battery, motor, gearbox, steering assembly, passenger, seat, and air conditioner. The static physical test is carried out in turn according to the sequence number. After the loading is completed, the unloading is done in the opposite way and repeated twice.

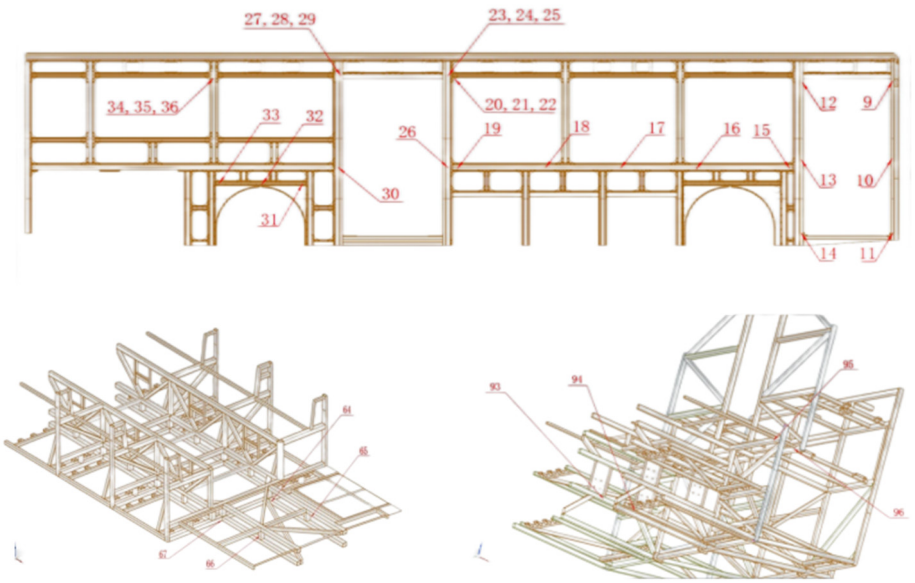

Figure 5. Some measurement points on the upper-frame.

The test is carried out in the pilot plant of an enterprise, and the test prototype and equipment are shown in Figure 6.

Figure 6. Test prototype and equipment.

In order to ensure the validity of the measurement results, the equation for calculating the effective strain is as follows:

$$\varepsilon = \varepsilon_{aL} - \frac{\varepsilon_{bL}+\varepsilon_{aU}}{2} \tag{1}$$

where ε_{aL} is strain value after loading; ε_{bL} is strain value before loading; ε_{aU} is strain value after unloading.

According to Hooke law, the stress has the following formulation:

$$\sigma_1 = E\varepsilon \tag{2}$$

In addition, a small number of strain gauges are also used. The calculation of strain is based on the following equation, which can be derived from two principal strains:

$$\varepsilon_{1,2} = \frac{E}{2}\left[\frac{\varepsilon_0+\varepsilon_{90}}{1-\mu} \pm \frac{1}{1+\mu}\sqrt{(\varepsilon_0-\varepsilon_{90})^2+(2\varepsilon_{45}-\varepsilon_0-\varepsilon_{90})^2}\right] \tag{3}$$

The main strain direction is:

$$\tan 2\alpha_0 = \frac{2\varepsilon_{45}-\varepsilon_0-\varepsilon_{90}}{\varepsilon_0-\varepsilon_{90}} \tag{4}$$

where $\varepsilon_{0°}$, $\varepsilon_{45°}$, $\varepsilon_{90°}$ are the strain values in the direction of 0°, 45°, and 90° in the strain gauges respectively; μ is Poisson's ratio; E is the modulus of elasticity and α_0 is the angle formed by the main strain line and the 0° line.

Table 1. Comparison between simulation calculation and physical test results.

Measurement points	Test values /MPa	Simulation values /MPa	Errors /%
9	10.07	10.21	1.4
12	-13.23	-13.66	3.3
18	2.40	2.58	7.5
26	14.76	15.08	2.2
38	13.19	13.51	2.4
39	12.92	12.84	0.6
40	-11.51	-11.35	1.4
46	-15.56	-15.41	1.0
56	-7.11	-6.93	2.5
59	32.73	28.71	12.3
63	23.60	24.56	4.1
65	-20.94	-18.86	9.9
75	34.26	34.36	0.3
84	38.18	34.75	8.9
86	28.67	28.11	2.0
99	-24.57	-24.68	0.4

The test values of each measurement point are compared with the FE analysis values under the

static full-load bending condition, and only some of the measurement points are listed for comparison. From Table 1, it can be seen that the test and simulation values of most of the points are basically consistent, except for some points with large errors. On the one hand, the error is caused by the difference between the simplification of the FE model and the actual body structure; on the other hand, the difference between the loading position of the load in the test process and the loading position in the simulation model. The results show that the error of one point is more than 10%, and the other simulation results agree well with the test results. Therefore, the FE model is considered to be effective for subsequent design optimization.

4. MOO of body skeleton

In the modular design, the bus's upper-frame has been made of lightweight aluminum alloy. However, the total mass of the bus still does not meet the weight reduction target. In order to further reduce the overall mass without affecting the original strength of the body, the proposed MOO method is applied for the lightweight design of the bus structure.

4.1. Sensitivity analysis

Before optimizing the bus structure, appropriate design variables must be chosen. Since the lower-frame of the bus body is the main load-carrying component and is made of pure steel, there is plenty of room for optimization.

Suitable variables can be selected from the lower-frame to optimize the body structure. The lower-frame, which contains over 600 components, is divided into four parts: front, middle, middle-rear and rear part. If the thickness of each part is taken as the variable, it will make the optimization results difficult to converge. Therefore, the optimization variables are processed in two steps: grouping and sensitivity analysis before optimization.

The symmetrical structure can be taken as a variable group according to the structural characteristics of the bus body. Based on this principle, the lower-frame structure was divided into 30 groups. The grouping of the lower-frame is shown in Figure 7, where those with the same color are combined into one group.

The following grouping of variables is based on the symmetry of the bus lower-frame structure. In order to further reduce the number of design variables and improve the optimization efficiency, the sensitivity analysis is used to seek the correlation between the structural performance response of the bus body and the variable parameters of the component thickness. Based on the sensitivity analysis, the response of the body structure performance to the thickness variable is found. The greater the response value, the more sensitive the component thickness influence on the response.

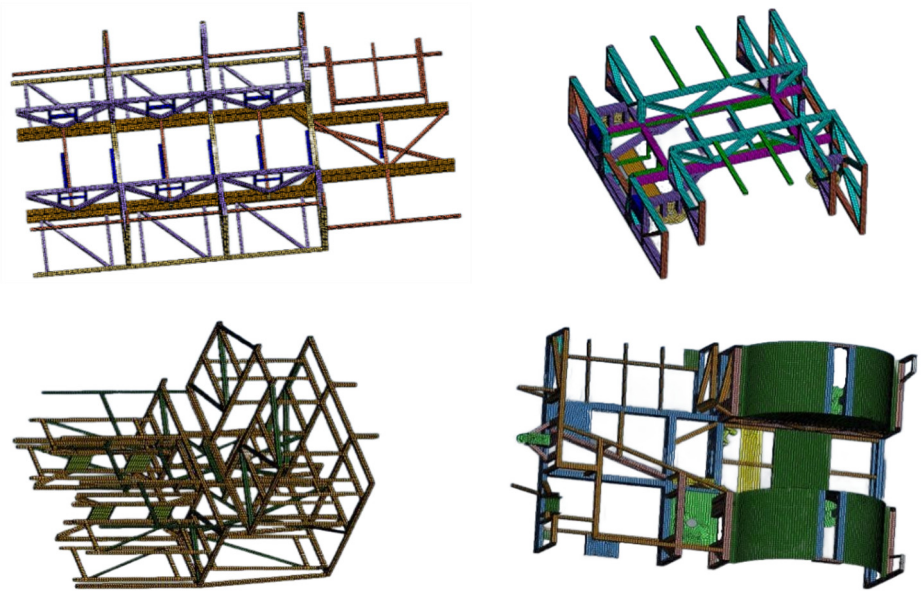

Figure 7. Variable grouping for bus lower-frame.

To ensure that the structural performance of the bus is minor changes, the variables with high mass sensitivity but negligible effect on structure performance should be selected for optimization design. In practice, the components with high mass sensitivity will be ignored because their sensitivity to other responses is also high. Properly reducing the thickness of these variables will make the reduction of other performances within an acceptable range. Therefore, the relative sensitivity analysis method can be used to find out the relative sensitivity of each performance of the body structure to mass. The optimization design is carried out by selecting components with relatively low sensitivity and taking the thickness of these components as a variable.

With the bus frame mass as the objective function and the first-order torsion frequency and bending stiffness (replaced by the displacement of the maximum displacement point under bending conditions) as the constraint functions, the relative sensitivity Ft/M of the first-order torsion frequency to the mass and the relative sensitivity Kb/M of the bending stiffness to the mass are calculated. The results are shown in Figure 8 and Figure 9, respectively. Excluding the 15 components with higher sensitivity, 15 variables with lower relative sensitivity values are selected with numbers 3, 4, 5, 6, 7, 8, 13, 16, 23, 24, 26, 27, 28, 29, 30, whose first-order torsional frequency and bending stiffness relative sensitivity values are less than 1, because their thickness changes are sensitive to the mass rather than first-order torsion frequency.

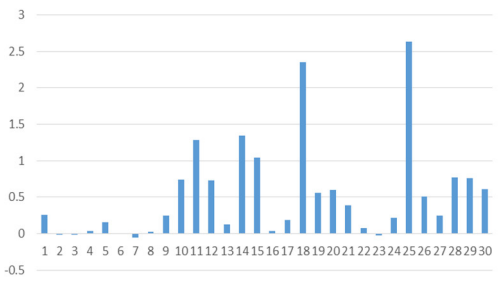

Figure 8. Ft/M sensitivity of body frame.

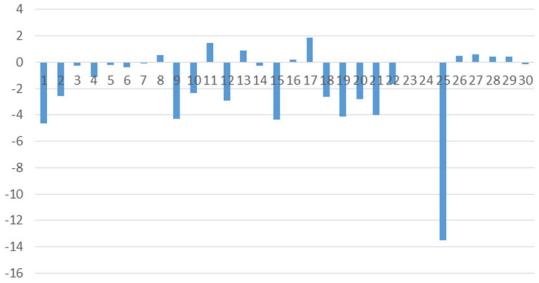

Figure 9. Kb/M sensitivity of body fram.

*4.2. S*ampling of test data

A sample of the design variables space as a training data set is generated by DOE. The DOE techniques include full factorial design, optimal Latin hypercube design, uniform design, orthogonal arrays, central composite design, factorial design, and Hamosilei sampling design, etc.

The Hamosilei sampling design has the advantage of requiring fewer samples to provide a reliable design for the output results. It has good uniform distribution in K dimensional hypercube. Therefore, the Hamosilei sampling design is used in this paper to sample 200 times in the sample space. Then the sample data were used for simulation analysis. Based on the calculated data, an approximate model of mass, stiffness, and mode is fitted.

4.3. RBF approximate model

The RBF is used in this study to approximate real structural performance criteria such as body strength, stiffness, torsion frequency, and mass, which significantly reduces the number of FE runs and thus improves optimization efficiency.

The RBF is a method of fitting multivariate functions by using discrete data. It is based on the radial function as the basis function and is constructed by linear superposition [14,15]. Its basic form is:

$$\hat{y}(x) = \sum_{i=1}^{n} \omega_i \, \phi(r_i) \tag{5}$$

where $r_i = \|x - x_i\|$ is the Euclidean distance, that is, the distance between x and the sample point x_i in the design space; ω_i is the weighting factor for the basis function;n is the number of the basic functions; ϕ is the basis function.

As the main bearing structure, the bus body frame must have enough stiffness to ensure the requirements of assembly. Enough sufficient strength is demanded to ensure the fatigue life. And dynamic characteristics should also be reasonable to improve occupant comfort. The stiffness of the bus body mainly includes bending stiffness and torsion stiffness. The torsion stiffness is mainly considered in this paper. To fit the approximate model of the bus, the front wheel shock absorber support point is shifted to the torsional stiffness of the bus. In the modal analysis of the bus body, the low-order modal frequencies are considered, so the modal approximation model is used to fit the first-order bending frequency and the first torsion frequency of the bus body.

There are features of the RBF model, which has better nonlinear approximation than the Kriging model. It is found that RBF provides fast convergence and stable results under the convergence

condition. Therefore, RBF is used to build the approximate models of body mass, torsional stiffness, torsional frequency, and first-order bending frequency.

By determining the coefficient R^2, the accuracy of the RBF model is validated.

$$R^2 = \sum_{i=1}^{h}(\hat{l}_i - \bar{l})^2 / \sum_{i=1}^{h}(l_i - \bar{l})^2 \tag{6}$$

where $\bar{l}$ is the mean of the response to the Y sample point; $\hat{l}_i$ is the response value of the approximate model at the first sample point.

The coefficient of determination R^2 is [0, 1]. And the closer the value is to one, the more accurate the approximate model. An additional 10 selected samples are used to validate the accuracy of RBF model. The R^2 values of body mass, torsional stiffness, torsion modal frequency and the first bending mode frequency are 0.995, 0.982, 0.953, 0.946, respectively. The coefficient of determination of each model is larger than 0.94, which can meet the requirement of accuracy.

4.4. MOO design

The MOO problem is significantly different from the single-objective optimization problems. Typically, MOO problem does not only have a single solution. Instead, there is a set of solutions that reflect different levels of trade-offs among objectives. The MOO problem can be expressed mathematically as follows:

$$\begin{aligned} min \quad & f(x) = \{f_1(x), f_2(x), \cdots, f_k(x) \\ st. \quad & g_p(x) \le 0; p = 1,2,\cdots l \\ & h_q(x) = 0; q = 1,2,\cdots, m \\ & x = [x_1, x_2, \cdots, x_n]^T \\ & x_{iu} \le x_i \le x_{id}, i = 1,2,\cdots, n \end{aligned} \tag{7}$$

where $f(x)$, $g_p(x)$, $h_q(x)$ are as the objective function, the inequality constraint and equality constraint function respectively; x as the design variables, k, l and m are as the number of objective function and constraint function inequality and equality constrained function respectively; x_{iu} and x_{id} are the upper and lower bounds for the design variables.

As a population-based method, a GA is well suited to solving MOO problems. It can search different regions of the solution space simultaneously, resulting in a diverse set of solutions for non-convex, discontinuous and multi-modal solution space puzzles. The multi-objective GA is an algorithm that explicitly uses Pareto-based ranking and division techniques to encourage search toward a true Pareto front while maintaining diversity in performance [16,17]. In this paper, the MOO design of the bus body frame structure is carried out, and the optimization process is shown in Figure 10.

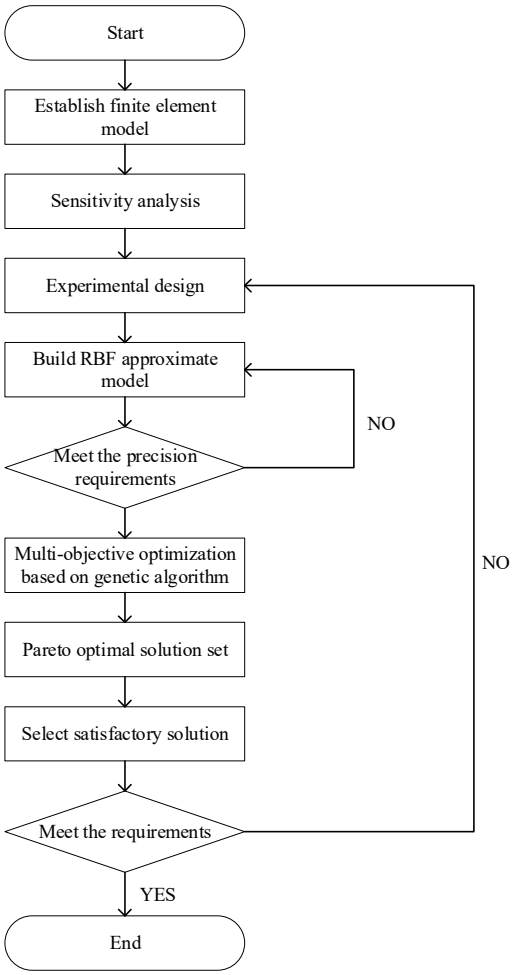

Figure 10. MOO process of car body framework.

The value range of design variables is defined as within plus or minus 50% of the initial thickness. In the MOO, the body skeleton mass and bending stiffness are used as the objective functions, the 15 sets of variable thickness parameters of the bus lower-frame are used as the design variables, and the first-order torsional modal frequency and the first-order bending modal frequency are used as the constraints. The mathematical model is expressed as follows:

$$\begin{aligned} min \quad & f(x) = \{f_1(x), |f_2(x)|\} \\ st. \quad & k_t(x) \geq 5.0; k_b(x) \geq 12.0 \\ & X = [x_1, x_2, \cdots, x_n]^T \\ & 0.5x_0 \leq x_i \leq 1.5x_0 \\ & i = 1,2,\cdots,15 \end{aligned} \tag{8}$$

where $f(x)$ is as the objective function, $f_1(x)$ and $f_2(x)$ are respectively the quality of body frame and the torsional rigidity of the objective function; $k_t(x)$ and $k_b(x)$ are the first-order torsion modal frequency and the first bending mode frequency constraint function respectively; x_i is the design variables of bar's thickness.

According to the above mathematical model, MOO based on GA is used to optimize with the Hyperstudy software. The Pareto optimal solution set of multi objective optimization is obtained, as is shown in Figure 11.

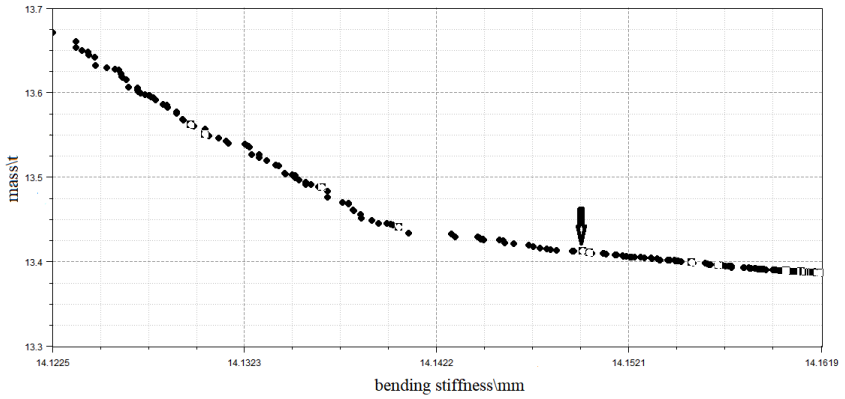

Figure 11. Pareto fronts of optimal solution set.

In the Pareto optimal solution set of Figure 11, it can be found that the fluctuation range of bending stiffness is small, while the fluctuation range of body frame mass is large. As long as a small amount of bending stiffness is sacrificed, a more satisfactory reduction of body structure mass can be achieved. Therefore, considering these two objectives, the solution indicated by the arrow in Figure 11 is selected as the final optimization solution. The best selected values of mass and bending stiffness are shown to be 13.4125 and 14.1497, respectively.

4.5. Comparison and analysis of performance before and after optimization

The thickness values of initial design and optimized design are shown in Table 2.

Table 2 Thickness values of initial design and optimized design.

Variable number	Initial design /mm	Optimal design /mm
3	7.0	5.5
4	10.0	9.5
5	6.0	8.5
6	8.0	6.5
7	5.0	5.0
8	1.5	0.5
13	6.0	3.5
16	4.0	2.0
23	10.0	5.0
24	6.0	3.0
26	2.0	1.0
27	3.0	1.5
28	4.0	2.0
29	1.5	0.5
30	2.0	1.0

In order to verify the structural performance of the bus skeleton after optimization, the validity of the MOO is verified by comparing the first-order torsional frequency of the bus body skeleton and the maximum stress under the bending condition. Figure 12 shows the maximum stress cloud diagram under the bending condition, and Figure 13 shows the first-order torsion frequency of the initial design and the optimal design.

The comparison results of the structural performance of the body frame before and after optimization are shown in Table 3. As shown in Table 2, the thickness of design variables is reduced to different degrees through optimization design. As can be seen from Figures 12, 13 and Table 3, the mass of the bus frame has changed from 4053 kg to 3883 kg through the optimization design. The mass of the frame has been reduced by 170 kg, and the lightweight ratio has reached 4.2%.

After optimization design, the maximum strain and maximum stress in bending conditions are not much changed compared with the initial design. The maximum stress in the torsion condition is reduced by 3.4 Mpa compared with the initial design. And the first-order torsion frequency and first-order bending frequency in modal performance have not changed significantly from the initial design. This is because the thickness change of the design variables shown in Table 2 has little effect on the torsion frequency of the body, but the thickness change has a greater impact on the body weight. In general, the lightweight effect of the bus body frame through MOO design is significant, and the structural performance of the bus still meets the design requirements of the bus.

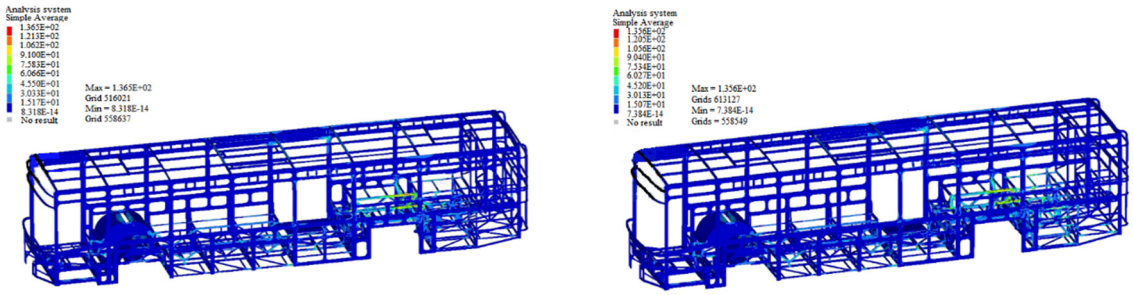

a) Initial design b) Optimal design

Figure 12. Maximum stress cloud diagram under the bending condition in before and after optimization condition.

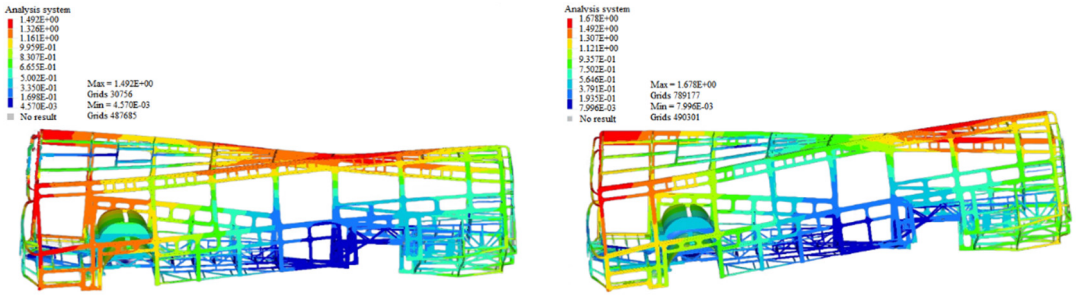

a) Initial design b) Optimal design

Figure 13. First order torsional frequency cloud diagram.

Table 3 Comparison of initial design and optimization design results.

Performance indicators	Initial results	Optimization results	Value change	Variation (%)
Bus frame quality /kg	4053	3883	-170	4.2
Maximum strain for bending conditions /mm	14.18	14.15	-0.03	0.2
Maximum stress in bending condition /MPa	136.5	135.6	-0.9	0.6
Maximum stress for torsional conditions /MPa	240.1	237.5	-3.4	1.4
First-order torsion frequency /Hz	5.56	5.632	0.07	1.2
First-order bending frequency /Hz	12.14	12.54	0.40	3.2

5. Conclusions

1) The frame structure body of the 12-meter pure electric bus adopted the combined design of steel and aluminum alloy material. On the basis of the traditional all-steel bus, the upper-frame structure used aluminum alloy material instead of steel. Compared with the traditional all-steel body structure, the mass of the frame on the body was reduced from 3905 to 2404 kg, with a mass reduction ratio of 38.4%.

2) The MOO design method based on GA and RBF models was used to optimize the bus frame structure. The optimization design analysis clearly showed that the optimized structure not only met the structural performance requirements, but also reduced the frame mass by 170 kg compared with the original design; and the lightweight ratio reaches 4.2%.

3) The steel-aluminum lightweight body and MOO method proposed in this paper, which provide an excellent idea for the mass reduction design of pure electric buses. It has broad application prospects in urban electric buses and some large motors, such as electric agricultural harvesters and household electric vehicles. This work can also provide a reference for the design of future pure aluminum electric buses.

4) The combination of welded and bolted riveted body connection was used in the FE model and was reasonably simplified in the FE software. However, in reality, modern bus frames have more complex connections. Furthermore, while the lightweight goal was achieved using the MOO method, the improvement of the multi-objective GA itself was not considered. In the future, more connection methods can be selected based on the body parts and bus types, and the multi-objective GA can be improved to achieve better results.

Acknowledgments

This work is supported by Anhui Provincial Development and Reform Commission's new energy vehicle and intelligent network connected automobile industry technology innovation project.

Conflict of interest

We declare there is no conflicts of interest.

References

1. L. Yu, X. Gu, L. Qian, P. Jiang, W. Wang, M. Yu, Application of tailor rolled blanks in optimum design of pure electric vehicle crashworthiness and lightweight, *Thin-Walled Struct.*, **161** (2021), 107410. https://doi.org/10.1016/j.tws.2020.107410
2. S. Baeka, G. Y. Go, J. W. Park, J. Song, H. Lee, S. J. Lee, et al., Microstructural and interface geometrical influence on the mechanical fatigue property of aluminum/high-strength steel lap joints using resistance element welding for lightweight vehicles: experimental and computational investigation, *J. Mater. Res. Technol.*, **17** (2022), 658–678. https://doi.org/10.1016/j.jmrt.2022.01.041
3. S. B. Lu, W. B. Jiang, W. J. Zuo, Size and morphology crashworthiness optimization for automotive frontal structures using equivalent static loads method, *J. Vibr. Shock*, **37** (2018), 56–61. https://doi.org/10.13465/j.cnki.jvs.2018.07.009
4. H. Zhao, S. Wang, X. Li, Z. Pang, G. Zhang, Optimization for side structure of vehicle based on FEA, *Procedia Comput. Sci.*, **208** (2022), 196–205. https://doi.org/10.1016/j.procs.2022.10.029
5. D. Jasoliya, D. B. Shah, A. M. Lakdawala, Topological optimization of wheel assembly components for all terrain vehicles, *Mater. Today Proc.*, **59** (2022), 878–883. https://doi.org/10.1016/j.matpr.2022.01.221
6. X. Xu, Y. Zhang, X. Wang, J. Fang, J. Chen, J. Li, Searching superior crashworthiness performance by constructing variable thickness honeycombs with biomimetic cells, *Int. J. Mech. Sci.*, **235** (2022), 107718. https://doi.org/10.1016/j.ijmecsci.2022.107718
7. D. Xie, L. Chen, L. Liu, L. Chen, H. Wang, Actuators and sensors for application in agricultural robots: a review, *Machines*, **10** (2022), 913. https://doi.org/10.3390/machines10100913
8. A. Ariyarit, P. Katasila, T. Srinaem, W. Sukkhanthong, The multi-objective design optimization of automated guided vehicles car structure using genetic algorithms, in *2020 IEEE 11th International Conference on Mechanical and Intelligent Manufacturing Technologies (ICMIMT)*, (2020), 103–107. https://doi.org/10.1109/ICMIMT49010.2020.9041222
9. Z. Xiang, Z. Zhu, Multi-objective optimization of a composite orthotropic bridge with RSM and NSGA-II algorithm, *J. Constr. Steel Res.*, **188** (2022), 106938. https://doi.org/10.1016/j.jcsr.2021.106938
10. Z. Zhang, X. Jia, T. Yang, Y. Gu, W. Wang, L. Chen, Multi-objective optimization of lubricant volume in an ELSD considering thermal effects, *Int. J. Therm. Sci.*, **164** (2021), 106884. https://doi.org/10.1016/j.ijthermalsci.2021.106884
11. Y. Ji, Z. Yang, J. Ran, H. Li, Multi-objective parameter optimization of turbine impeller based on RBF neural network and NSGA-II genetic algorithm, *Energy Rep.*, **7** (2021), 584–593. https://doi.org/10.1016/j.egyr.2021.10.003
12. J. Vorderbrüggen, D. Köhler, B. Grüber, J. Troschitz, M. Gude, G. Meschut, Development of a rivet geometry for solid self-piercing riveting of thermally loaded CFRP-metal joints in automotive construction, *Compos. Struct.*, **291** (2022), 115583. https://doi.org/10.1016/j.compstruct.2022.115583

13. P. K. Mallick, Joining for lightweight vehicles, in *Materials, Design and Manufacturing for Lightweight Vehicles*, (2011), 275–308. https://doi.org/10.1533/9781845697822.2.275
14. Y. Niu, J. Shao, J. Xiao, W. Song, Z. Cao, Multi-objective evolutionary algorithm based on RBF network for solving the stochastic vehicle routing problem, *Inf. Sci.*, **609** (2022), 387–410. https://doi.org/10.1016/j.ins.2022.07.087
15. G. E. Tsekouras, J. Tsimikas, On training RBF neural networks using input–output fuzzy clustering and particle swarm optimization, *Fuzzy Sets Syst.*, **221** (2013), 65–89. https://doi.org/10.1016/j.fss.2012.10.004
16. A. Konak, D. W. Coit, A. E. Smith, Multi-objective optimization using genetic algorithms: a tutorial, *Reliab. Eng. Syst. Saf.*, **91** (2006), 992–1007. https://doi.org/10.1016/j.ress.2005.11.018
17. F. Chi, Y. Xu, Building performance optimization for university dormitory through integration of digital gene map into multi-objective genetic algorithm, *Appl. Energy*, **307** (2022), 118211. https://doi.org/10.1016/j.apenergy.2021.118211

AIMS Press